Multispectral UAV-Based Monitoring of Cassytha Filiformis Invasion in Xisha Islands

Yuhan Xie, Wenjin Wu, Xinwu Li, Jiankang Shi, Tong Yu, and Xiaohui Sun

***Abstract*—Currently, numerous studies have reported that the invasion of *Cassytha filiformis* has affected both above and below ground communities, resulting in difficulties in the growth of original vegetation. Meanwhile, *Cassytha filiformis* was observed on the Xisha Islands in recent years which brings up the importance of monitoring its invasion to protect the biodiversity of the island. Nonetheless, to effectively monitor *Cassytha filiformis* at finer regional scales, there is a pressing need for centimeter-level resolution, a level of precision that current satellite sensors find challenging to attain in a consistent manner. Therefore, we adopted a DJI Phantom 4 unmanned aerial vehicle with five multispectral bands and centimeter-level spatial resolution to overcome this problem. An advanced deep learning network is employed to identify the invasion in Xisha Islands for three different time periods. Results show that the area of *Cassytha filiformis* on Bei Island increased from 211.8 m^2 in April 2020 to 458.6 m^2 in April 2021, and dropped to 112.8 m^2 in July 2021, while that on Ganquan Island changed from 1996.9 m^2 in April 2021 (dry season) to 1275.9 m^2 in July 2021 (wet season). By incorporating climatic indicators, we further found that *Cassytha filiformis* in both Bei Island and Ganquan Island favors dry climate and its large area invasion in 2021 was possibly caused by a drought event.**

***Index Terms*—Cassytha filiformis, deep learning (DL), unmanned aerial vehicle (UAV) remote sensing, vegetation invasion, Xisha Islands.**

I. Introduction

INVASIVE species pose a significant threat to biodiversity and ecosystem stability worldwide. Wherein, *Cassytha filiformis* is a parasitic and invasive plant with leafless, climbing, twining, vine-like, autoparasitic and plant hyperparasitic phanerogams (seed-bearing plant) in the plant family Lauraceae [1] (see Fig. 1). It is widely distributed in tropical regions [2] and is known to parasitize at least 26 species of vascular and seed-bearing plants [3]. *Cassytha filiformis* seeds are dispersed by water, wind, or animals, which are also able to survive for more than two months without a host until it infects the host plant [4]. Besides, the seeds attack and invade the bast and xylem of the host plant to extract nutrients and water from the cells [5], resulting in lethal damage to the host cells and their metabolic processes. The host plants may die for a long time, while severe infestation may affect plant regrowth and threaten the ecosystem. There were a few studies currently monitoring the invasion of *Cassytha filiformis*, and most of them indicate that the *Cassytha filiformis* has numerous hosts and its invasion is significant in tropical coastal areas. Among them, Rohani et al. reported parasitic plants in the coast of Setiu, Terengganu. They recorded a total of seven invasive plants in these two areas and found that *Cassytha filiformis* was dominant, widespread and highly invasive in both locations [6]. Kidunda et al. [7] studied the phenomenon of *Cassytha filiformis* invasion in cashew trees in Tanzania and found that cashew and mango crops were seriously affected by *Cassytha filiformis* invasion and the phenomenon of *Cassytha filiformis* invasion was more serious in lower latitude areas. The Ecosystem Action Plan for the U.K. Indian Ocean Territory [8] indicates that *Cassytha filiformis* is common on 32 of the 55 islands of the Chagos Archipelago and regularly infests the islands, but its impact on the ecological environment of the area is relatively small.

The Xisha Islands locate in the northwest of the South China Sea, are a group of small tropical islands of high strategic importance to China. The ecological and environmental conditions on the Xisha Islands are of great concern [9], [10]. Being far from the mainland and mostly uninhabited, the Xisha Islands are still relatively pristine with simple and fragile vegetation communities [10]. Invasion of invasive species such as *Cassytha filiformis* will likely pose ecological risks to the Xisha Islands and have significant impacts on the islands' fragile ecosystem.

Manuscript received 11 July 2023; revised 7 September 2023, 8 September 2023, and 11 October 2023; accepted 20 October 2023. Date of publication 7 November 2023; date of current version 4 December 2023. This work was supported in part by the National Key Research and Development Program of China under Grant 2021YFF0704400, and in part by the National Natural Science Foundation of China under Grant 42276241. *(Corresponding authors: Wenjin Wu; Xinwu Li.)*

Yuhan Xie is with the Key Laboratory of Digital Earth Science, Aerospace Information Research Institute, Chinese Academy of Sciences, Beijing 100045, China, also with the International Research Center of Big Data for Sustainable Development Goals, Beijing 100045, China, and also with the University of Chinese Academy of Sciences, Beijing 100045, China (e-mail: xyhan_1@163.com).

Wenjin Wu is with the International Research Center of Big Data for Sustainable Development Goals, Beijing 100045, China, and also with the Key Laboratory of Digital Earth Science, Aerospace Information Research Institute, Chinese Academy of Sciences, Beijing 100045, China (e-mail: wenjin.wu.happy@gmail.com).

Xinwu Li is with the International Research Center of Big Data for Sustainable Development Goals, Beijing 100045, China, also with the Key Laboratory of Digital Earth Science, Aerospace Information Research Institute, Chinese Academy of Sciences, Beijing 100045, China, and also with the Key Laboratory of Earth Observation, Hainan Institute, Institute of Aerospace Information Research, Chinese Academy of Sciences, Sanya 100045, China (e-mail: xwli@cbas.ac.cn).

Jiankang Shi is with the Hainan Academy Research of Environmental Sciences, Haikou 571126, China (e-mail: stanking16888@163.com).

Tong Yu is with the College of Agricultural and Life Sciences, University of Wisconsin Madison, Madison, WI 53706-1380 USA (e-mail: yutong@aircas.ac.cn).

Xiaohui Sun is with the Qilu Research Institute, Aerospace Information Research Institute, Chinese Academy of Sciences, Jinan 100045, China (e-mail: sunxh01@aircas.ac.cn).

Digital Object Identifier 10.1109/JSTARS.2023.3330768

Fig. 1. *Cassytha filiformis* invades wild plants in nature in June 2011 by NIKON D200.

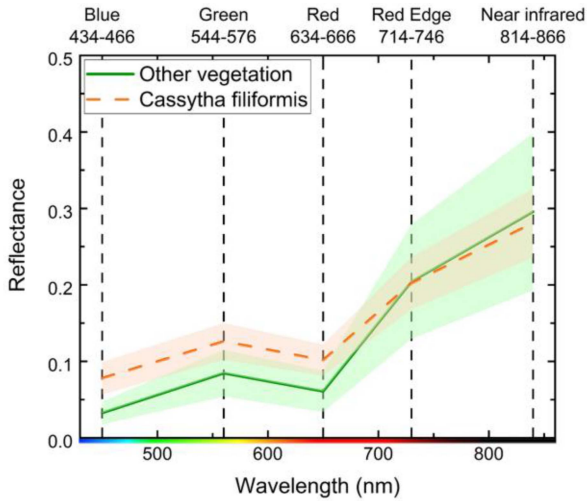

Fig. 2. Spectral reflectance curves of *Cassytha filiformis* and other vegetation on Guanquan Island from DJI Phantom 4 multispectral imagery (April 2021). The curve for *Cassytha filiformis* is derived from 1800 typical pixels, and the curve for other vegetation was obtained from 1800 pixels of representative vegetation species on Xisha Island including *Sophora tomentosa*, *Guettarda speciosa L.*, *Scaevola sericea Vahl*, *Heliotropium foertherianum,* and *Stachytarpheta jamaicensis*. Shaded areas indicate standard deviations around the mean values.

Cai et al. [11] found that the invasion of *Cassytha filiformis* changed the structure of the invaded communities and triggered changes in soil properties. Islands are relatively simple ecosystems, and the harmful effects of invasive plants are particularly evident on islands [12], where even islands with high biodiversity have difficulty resisting invasive vegetation. Invasive vegetation often leads to vegetation degradation [13] and biodiversity reduction in island ecosystems [14]. Currently, forest vegetation in Xisha Islands becomes less healthy because of invasive plants [10]. Therefore, monitoring the growth dynamics of *Cassytha filiformis* and studying its dispersal factors are essential for the conservation of the Xisha Islands ecosystem and may also provide a theoretical basis for the prevention and control of *Cassytha filiformis* invasion.

Approaches to monitor vegetation invasion usually based on field surveys. Although field surveys provide precise outcomes, they are laborious, time-consuming, and inadequate for continuous monitoring purposes. With the rapid development of remote sensing technology, many ecologists have conducted large-scale spatial and temporal studies of invasive plants using satellite imagery [15], [16], [17], [18], [19], [20]. However, it requires centimeter-resolution to conduct the monitoring of *Cassytha filiformis* at small regional scales which is hard to achieve with satellite sensors. Moreover, since the Xisha Islands are located in the tropics and are cloudy throughout the year, satellite optical images are easily obscured by clouds, resulting in missing images. With the application and development of unmanned aerial vehicle (UAV) remote sensing technologies, UAV observation has become an important complementary tool to traditional field observation. It has been used in many fields, such as plant growth monitoring, ecological environmental monitoring, and natural disaster investigation [21], [22], [23], [24], [25], [26], [27], [28]. The UAV platform is not impeded by clouds and has an extended flight duration, along with the ability to capture images at a higher spatial resolution [29]. This makes it possible to monitor changes in the growth of *Cassytha filiformis* [30]. Specifically, in high-resolution imagery, *Cassytha filiformis* exhibits distinct morphological features. It possesses a slender, vine-like structure that often appears as gray-white or gray-brown in true-color images. We extracted 1800 typical pixels each from *Cassytha filiformis* and other vegetation on Ganquan Island to derive their respective spectral curves (see Fig. 2). There is a noticeable difference between the spectral curves of the *Cassytha filiformis* and other vegetation. This difference, especially evident within the blue, green and red bands, the reflectance of *Cassytha filiformis* is significantly higher than that of other vegetation. In the near-infrared band, the reflectance of *Cassytha filiformis* is slightly lower than that of other vegetation. These unique characteristics are crucial for accurate identification and monitoring using UAV.

In this article, our primary objective was to address the challenge of monitoring the invasion of *Cassytha filiformis* in the Xisha Islands using high-resolution UAV remote sensing imagery. Given the complexities of extracting invasive areas from centimeter-level images, we employed an advanced deep learning model. This model not only emphasizes spatial and spectral details in high-resolution imagery but also effectively tackles the sample imbalance issues commonly encountered in automatic classification due to limited datasets. To validate our approach, we identified the invasion patterns over three distinct time periods on two representative islands in the Xisha archipelago, integrating visual interpretation to refine and verify our findings. Moreover, our research delves deeply into the climatic drivers affecting the growth of *Cassytha filiformis*, specifically examining fluctuations between interannual and dry-wet seasons.

II. Materials and Methodology

A. Study Area

The Xisha Islands are located in the northwestern part of the South China Sea, southeast of Hainan Island, and belong to Sansha City, Hainan Province, China, which is among the

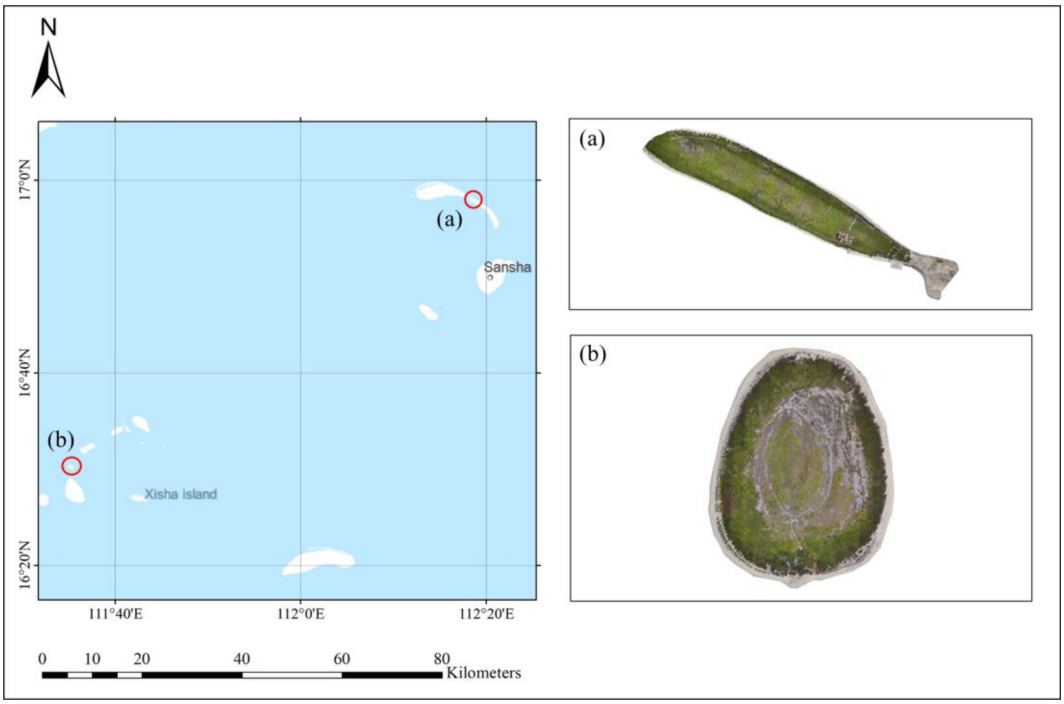

Fig. 3. Study area and remote sensing imagery. (a) Bei Island—True color band imagery acquired with DJI Phantom 4 in April 2021. (b) Ganquan Island—True color band imagery acquired with DJI Phantom 4 in April 2021.

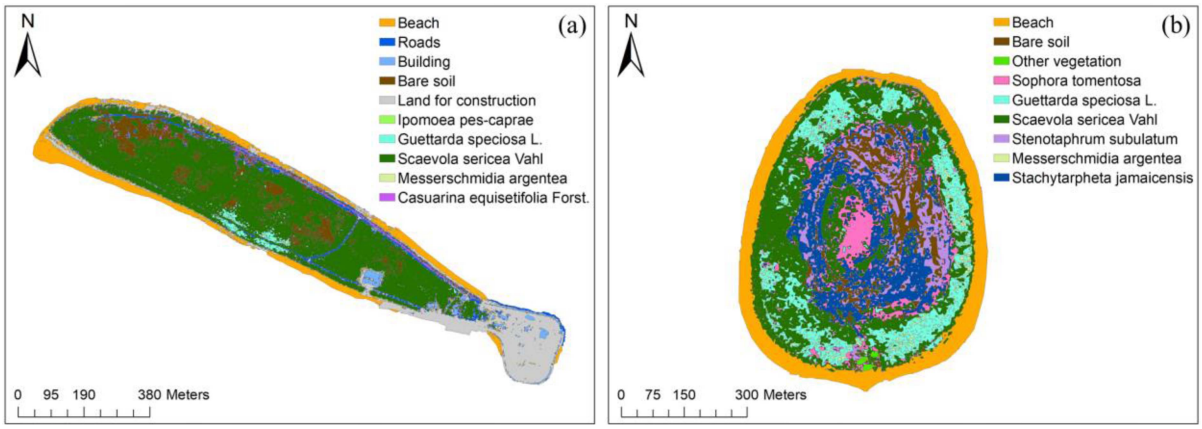

Fig. 4. Distribution of vegetation types in 2018 for (a) Bei Island, and (b) Ganquan Island: results derived from our previous classification efforts.

four major islands in the South China Sea. The Xisha Islands (15°47'∼17°08' N, 15°47'∼17°08' E) include 40 islands and reefs with a sea area of about 501,011m^2, consisting mainly the Yongle Islands and the Xuande Islands, and have a tropical monsoon climate with distinct dry and wet seasons. It is easy to be affected by disasters such as droughts, typhoons, and heavy rains. The data used in this study are obtained from Bei Island and Ganquan Island in the Xisha Islands, where *Cassytha filiformis* invasion have affected the local ecosystems (see Fig. 3).

The Bei Island is located in the Xuande Islands of the Xisha Islands and is the largest island of the Seven Linked Islands. It is 1500 m long and 350 m wide at its widest point, has an area of 0.4 km^2 with altitude of 3–4 m, is surrounded by sand dikes, and is uninhabited. The Bei Island is populated by *scrub*, and the main vegetation types are *Scaevola sericea Vahl*, *Casuarina equisetifolia Forst.,* and *Guettarda speciosa L.*, of which *Scaevola sericea Vahl* is widely distributed. As can be seen from the map of vegetation distribution in 2018 (see Fig. 4), which was obtained in our previous work, we classified the land types of the Xisha Islands in 2018 using UAV images. The area of *Scaevola sericea Vahl* is 0.17 km^2, and its proportion is 50.7%. We can also see that there is no *Cassytha filiformis* on Bei Island in 2018.

Ganquan Island is located in the western part of the Yongle Islands. The island is oval, 700 m long from north to south and 500 m wide from east to west, with an area of about 0.3 km^2. The island has evolved from a coral atoll into a grey sandy islet,

TABLE I
SPECTRAL BAND CHARACTERISTICS OF DJI PHANTOM 4 MULTISPECTRAL SENSOR

Band Name	Central Wavelength (nm)	Band Range (nm)
Blue	450	434–466
Green	560	544–576
Red	650	634–666
Red edge	730	714–746
NIR	840	814–866

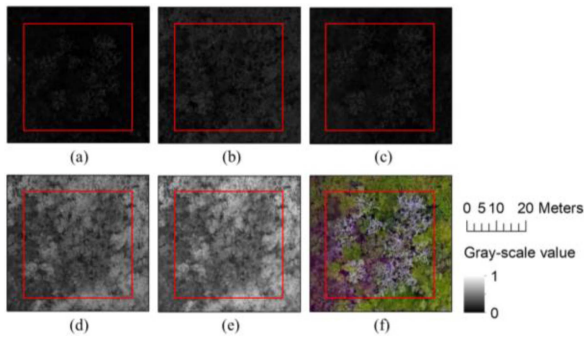

Fig. 5. Sample images in the DJI Phantom 4 imagery where *Cassytha filiformis* are highlighted in red. (a) Blue band. (b) Green band. (c) Red band. (d) Red edge band. (e) NIR band. (f) True color composition.

encircled by a coral reef. The central part of the island evolved from a desiccated lagoon lake. This central region is surrounded by a concentric forest belt, which in turn is bordered by a sandy ridge, presenting a concentric landscape. The island has a great diversity of vegetation, which mainly includes *Guettarda speciosa L.*, *Scaevola sericea Vahl*, *Stachytarpheta jamaicensis*, *Stenotaphrum subulatum,* and *Sophora tomentosa*. As shown in the 2018 vegetation distribution map, there is no *Cassytha filiformis* growing on the island. *Guettarda speciosa L.*, *Scaevola sericea Vahl*, *Stenotaphrum subulatum,* and *Stachytarpheta jamaicensis* are widely distributed, with the area of 0.05 km^2 (13.8%), 0.1 km^2 (29.4%), 0.03 km^2 (8.8%), and 0.05 km^2 (14.9%) respectively.

B. Source of Data

The primary data source for this study is multispectral imaging data from the DJI Phantom 4. Data were collected in April 2021, July 2021, and April 2020. The flight time of the drone is from 15:00 to 16:00, with good sunlight conditions and weak wind, and the spatial resolution of the images is 6.4 cm. The drone is equipped with six 1/2.9-inch complementary metal oxide semiconductor sensors, including one color sensor for accurate color imaging and five monochrome sensors for multispectral imaging, covering the blue, green, red, red-edge, and near-infrared bands (detailed information on the bands is given in Table I).

The multispectral light intensity sensor on the top of the fuselage captures the incident light intensity of the five bands in real time to compensate for imaging and provide more accurate multispectral information. Local grayscale images of the five multispectral bands are shown in Fig. 5, with the areas outlined in red showing the more distinct distribution of *Cassytha filiformis*. As can be seen, the *Cassytha filiformis* in the blue and red bands appear white in the grayscale image and are easier to distinguish than in the other bands.

Meteorological data were obtained from Xisha Islands for April 2020, April 2021, July 2021, and the same period as in previous years. These include daily mean temperature (°C), daily mean wind speed (m/s), daily precipitation data (mm) from 8 pm to 8 pm and daily potential evapotranspiration (mm). The primary sources for this data were the National Climatic Center and the National Oceanic and Atmospheric Administration (NOAA) operating systems. The averages for the corresponding periods in previous years were determined using data from 2000 to 2015. The Oceanic Niño Index (ONI) was obtained from the NOAA, which is derived from the sea surface temperature (SST) anomalies observed in the Niño 3.4 region, spanning across the central and eastern Pacific (5°N–5°S latitude and 120°–170°W longitude). To calculate the ONI, the monthly average SST of the Niño 3.4 region is first determined and compared with the long-term historical average of this region, yielding monthly SST anomalies. Subsequently, to diminish the impact of short-term fluctuations and more adeptly capture the climatic characteristics of El Niño or La Niña, a three-month moving average of these SST anomalies is derived, leading to the ONI value. NOAA's criterion for assessing El Niño is that the value of the ONI must be above 0.5 °C for at least five consecutive months, and if its value is below −0.5 °C for five consecutive months or more, it is classified as a La Niña event. Simultaneously, due to the slow spatial variation of climatic factors and the fact that the islands within our study area are situated in the same oceanic region, the climatic factors at a given time are remarkably consistent. As a result, our research did not emphasize the spatial differences of these climatic factors. Instead, we primarily focused on the temporal variations of these factors and analyzed their relationship with the invasive regions of *Cassytha filiformis*.

C. Methodology

The roadmap of this study is shown in Fig. 6. First, a dataset was created based on the DJI Phantom 4 images and the deep learning model was trained for *Cassytha filiformis* detection. After the automatic classification, we implemented visual check and modification to derive more accurate results. Vegetation indices of *Cassytha filiformis* was evaluated and we also analyzed the growth status and driving factors of *Cassytha filiformis* in dry and wet seasons respectively with meteorological data. Finally, the meteorological data were used to investigate the potential climate drivers for the spread of *Cassytha filiformis* in the Bei Island in April 2021. The detailed processing steps are described as follows.

1) Data Preprocessing: Due to different positions of spectral cameras on the DJI Phantom 4, there are offsets between the

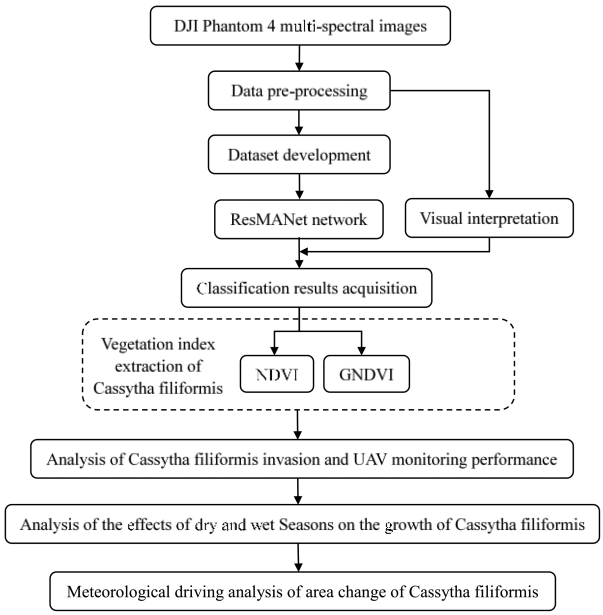

Fig. 6. Research roadmap.

captured images of each band which must be compensated for. We followed the P4 multispectral image processing guide [31] and the method proposed by Zhang [32] for fast radiometric correction of DJI P4M multispectral data. Key steps include band alignment and radiometric calibration. The image data were then imported into DJI Terra software to reconstruct two-dimensional (2-D) multispectral data, stitch and synthesize multispectral images, and crop them using island boundaries.

2) Vegetation and Meteorological Index Calculation: We employed the normalized difference vegetation index (NDVI) and the green normalized difference vegetation index (GNDVI) as metrics to assess the vitality of vegetation within *Cassytha filiformis* plots. The NDVI and GNDVI have been ubiquitously recognized and utilized due to their adeptness at discerning the differential reflectance between the red and near-infrared light of vegetation [33], [34], [35]. Vigorous vegetation predominantly absorbs most of the visible spectrum while reflecting a significant portion of the near-infrared range. This trend inversely transposes when vegetation is under stress or in suboptimal health, culminating in diminished NDVI and GNDVI values. Consequently, by examining the fluctuations in these indices across the dry and wet seasons, we aimed to better understand the seasonal influences on the growth of *Cassytha filiformis*. Additionally, the relative moisture index (MI) was selected to analyze the degree of humidity in the climate and explore the climate driving factors for the growth and changes of *Cassytha filiformis*.

1) Normalized Difference Vegetation Index NDVI has a strong linear relationship with vegetation cover and can be used to monitor seasonal and interannual variations in vegetation growth [36]. Its value ranges from −1.0 to 1.0. Zero value denotes bare ground and values close to 1.0 indicate pure vegetation. Negative values usually represent snow and water patches

$$\mathrm{NDVI} = \frac{\rho_{\mathrm{NIR}} - \rho_{\mathrm{RED}}}{\rho_{\mathrm{NIR}} + \rho_{\mathrm{RED}}} \tag{1}$$

where ρ_{NIR} is the NIR band reflectance and ρ_{RED} is the Red band reflectance.

2) Green Normalized Difference Vegetation Index The GNDVI is similar to the NDVI, but has better capacity to distinguish green vegetation from nonvegetation as it correlates better with chlorophyll contents [37], with values ranging from −1.0 to 1.0. A higher value of GNDVI correlates with higher levels of chlorophyll content.

$$\mathrm{GNDVI} = \frac{\rho_{\mathrm{NIR}} - \rho_{\mathrm{GREEN}}}{\rho_{\mathrm{NIR}} + \rho_{\mathrm{GREEN}}} \tag{2}$$

where ρ_{GREEN} is the Green band reflectance.

3) Moisture Index The MI is one of the indicators used to characterize the balance between precipitation and evapotranspiration over a period of time, and is suitable for drought monitoring during the growing season of vegetation. The higher value of MI means the climate is relatively humid.

$$\mathrm{MI} = \frac{P - \mathrm{PET}}{\mathrm{PET}} \tag{3}$$

where *P* is the precipitation during a certain period, measured in millimeters (mm), and PET is the potential evapotranspiration during a certain period, calculate by FAO Penman–Monteith method, measured in millimeters (mm). The Penman equation can be expressed as

$$E = \frac{\Delta\left(R_n - G\right) + \rho a \epsilon \sigma \left(T_s - T_a\right)}{\Delta + \gamma\left(1 + r_s / r_a\right)} \tag{4}$$

where E is the evaporation rate (usually in mm/day), Δ is the function of saturated vapor pressure with temperature, R_n is the net radiation, G is the soil heat flux, ρ is air density, a is the psychrometric constant, ϵ is the relative humidity of the air, σ is the Stefan-Boltzmann constant, T_s and T_a are the surface and air temperatures, respectively, γ is the psychrometric constant, r_s and r_a are the resistances of the surface and air, respectively.

3) Dataset Development: To train and validate the model, a *Cassytha filiformis* classification dataset was created. Large areas with distinct *Cassytha filiformis* characteristics were intercepted as the regions to be sampled in Bei Island and Ganquan Island of the Xisha Islands. Using ArcGIS software, we manually labeled the areas to be sampled within the UAV images, categorizing them into *Cassytha filiformis*, other vegetations types, and additional categories. Subsequently, we generated 2131 samples, each measuring 256 × 256 pixels, from the segmented images. To enhance the dataset, we augmented these samples using techniques such as 90°, 180°, and 270° rotations, mirroring, and color dithering, expanding the dataset to include 12 786 samples, each with dimensions of 256 × 256 pixels. This enriched dataset captures the unique attributes of ground targets within each sample. For analysis, we randomly split the dataset into training and validation sets at an 8:2 ratio using a specific function. The training set consists of 10 229 samples,

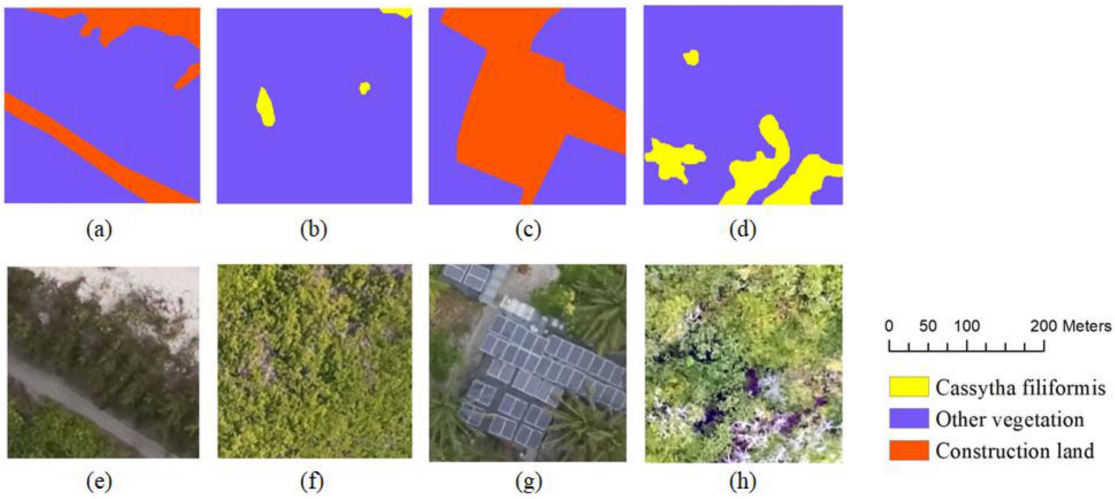

Fig. 7. Samples in the *Cassytha filiformis* classification dataset. (a)–(d) Labels. (e)–(h) Corresponding UAV image.

while the validation set comprises 2557 samples. Meanwhile, A few samples of the dataset are presented in Fig. 7.

4) Construction of the Deep Learning Model: Considering that the area of *Cassytha filiformis* is very small and it is not easy to distinguish it from other vegetation, we used the residual multiattentive network (ResMANet) proposed in our previous work [38]. ResMANet incorporates a multiscale convolutional neural network to extract features at different scales. Suitable for extracting features like *Cassytha filiformis*, which is scattered and relatively small in images. Additionally, it utilizes an attention mechanism to refine the feature map, emphasizing the spatial and spectral information of crucial features in high-resolution multispectral remote sensing images. To address the challenge of imbalanced data in small datasets, a joint loss function is constructed, using a two-stage network training strategy. The first stage involves the creation of a joint loss function through cross-entropy loss (CEL) and generalized Dice loss (GDL) (5). In the second stage, the focal loss is used to fine-tune the weights (8), directing the model to focus on training with sparse and challenging samples. Especially for rare and challenging categories like *Cassytha filiformis*, this loss function can help the model to learn and optimize better

$$\text{Joint Loss} = \text{GDL} + \text{CEL} \tag{5}$$

$$\text{GDL} = 1 - 2\frac{\sum_{l=1}^{m} w_l \sum_n r_{\text{ln}} p_{\text{ln}}}{\sum_{l=1}^{m} w_l \sum_n (r_{\text{ln}} + p_{\text{ln}})} \tag{6}$$

$$w_l = \frac{1}{\sum_{i=1}^{N} r_{\text{ln}}^2} \tag{7}$$

where, m represents the number of classes; N denotes the number of pixels; r_{ln} stands for the ground truth of category l at the nth pixel, while p_{ln} signifies the corresponding predicted probability; w_l represents the weight of each class.

$$\text{Focal loss} = -\sum (1 - p_t)^{\gamma} * T * \log p_t. \tag{8}$$

Moreover, γ is set to 2, T is the ground truth, and p_t represents the predicted probability. This approach helps mitigate the common sample imbalance problem, enhancing the model's performance on the classification task. Through these techniques, we aimed to achieve more accurate and reliable identification of *Cassytha filiformis*, facilitating effective monitoring and management of its invasion in the Xisha Islands.

The network uses an encoder-decoder structure that provides better recognition capability for features without detectable spatial features. The encoder contains five convolutional stages, and the feature extraction part includes two residual structures, namely "conv_block" and "identity_block." The convolution kernel of "conv_block" is set to be 1×1, 3×3, 5×5, and 7×7, to improve the recognition ability of features with insignificant spatial features. The decoder consists of an upsampling layer, a summation layer, and a convolution layer. After merging the input feature maps, the refined feature map obtained from the attention module is passed to the upsampling layer and then to the 3×3 convolutional layer to perform bilinear interpolation. The above steps are repeated to gradually restore the feature map to its original size and input it to the softmax layer for probabilistic prediction. The decoder integrates multiple layers of shallow features to compensate for the lack of position information in deep parts and improve the accuracy of delineating small objects. Following this, we utilized the sample set created from UAV imagery, inputted it into the ResMANet network for training, predicted the *Cassytha filiformis* on Bei Island in April 2020, April and July 2021, and Ganquan Island in April and July 2021 by using this model.

III. Result

A. Classification Performance Based on ResMANet and the UAV Dataset

Before performing the analysis, ResMANet was trained with the *Cassytha filiformis* classification dataset. During the training, the learning rate was set to 2×10^{-4}, the learning decay rate to 2×10^{-5}, the input of 16 images for each training, and the number of learning cycles to 120. We stopped training after the accuracy stopped improving, and the training accuracy stabilized

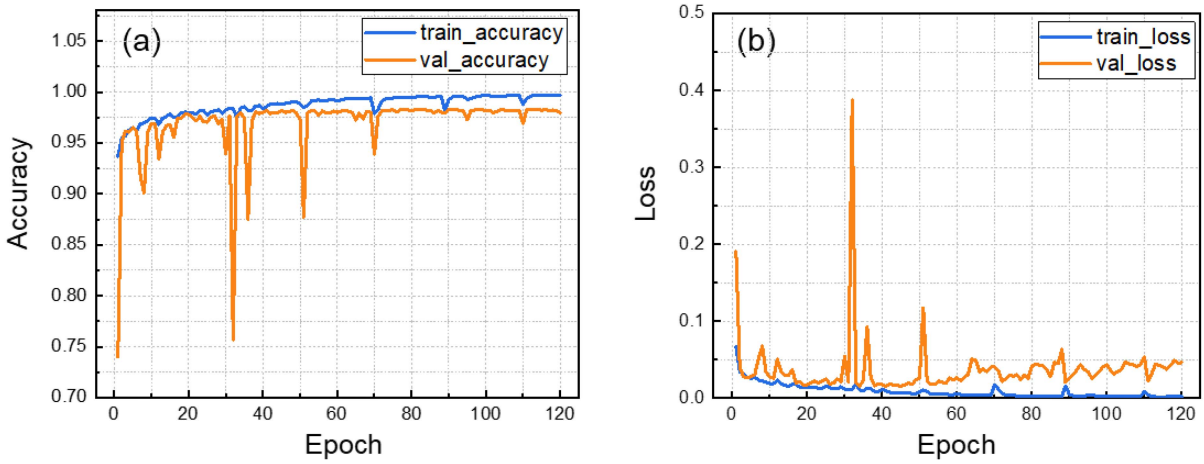

Fig. 8. Performance curves of the ResMANet model. (a) Accuracy curve, (b) loss curve.

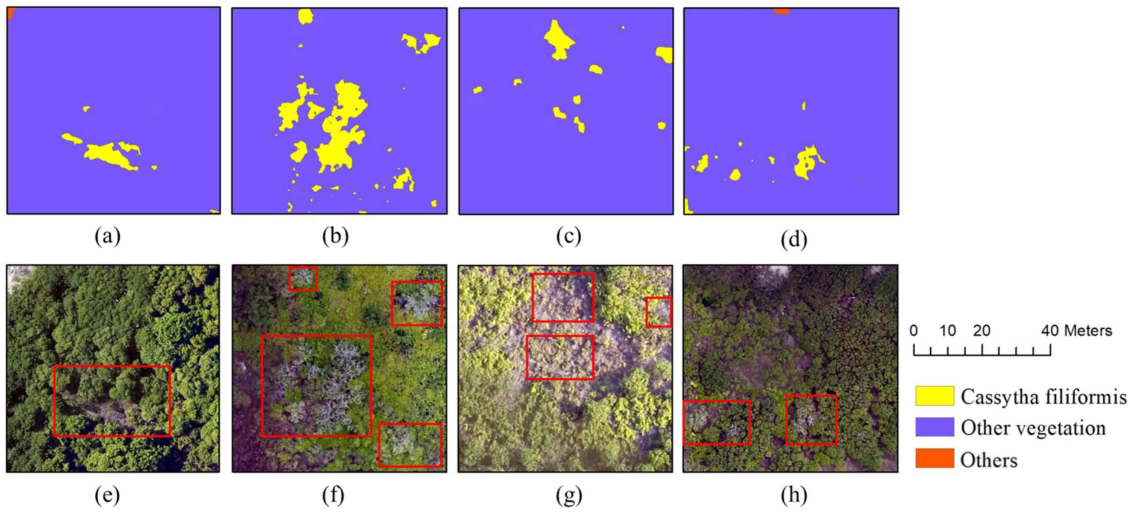

Fig. 9. Examples of classification details. (a)–(d) Result of the classification details, (e)–(h) Corresponding UAV image where *Cassytha filiformis* are highlighted in red frames.

after it increased to 99.7% which shows good training accuracy. The performance of ResMANet during the training is shown in Fig. 8. Through a prediction comparison, the 114th training result (99.76% accuracy) was selected as the model for further classification.

Examples of classification results are in Fig. 9. Among them, the red circle marks the *Cassytha filiformis* in the original image. From our visual observations during the field investigation, we can confirm that the locations and distributions of *Cassytha filiformis* as indicated in our classification results align well with our on-ground findings. The model generally exhibits proficiency in distinguishing *Cassytha filiformis* from other types of vegetation. However, there were some misclassifications observed, particularly with small-sized *Cassytha filiformis*. Nevertheless, the model effectively accomplishes the classification of the *Cassytha filiformis*, achieving satisfactory results. The original intention of this model design is to classify tropical forest regions. Through this experiment, we found that this model also showed good adaptability in monitoring *Cassytha filiformis* invasion in small tropical islands when combined with high-resolution UAV imagery. Recognizing the challenges associated with the small size of these vines, it is understandable that classification errors may occur. To address this, we conducted a visual interpretation of the misclassified areas and manually corrected the results. This additional step was taken to ensure the overall accuracy and reliability of the classification outcomes.

B. Results of Cassytha Filiformis Invasion Monitoring

Fig. 10 shows the classification results which demonstrate that both Bei Island and Ganquan Island were invaded by *Cassytha filiformis*. The area on Bei Island increased from 211.8 m^2 in April 2020 to 458.6 m^2 in April 2021, and then dropped to 112.8 m^2 in July 2021. The area on Ganquan Island decreased from 1996.9 m^2 in April 2021 to 1275.9 m^2 in July 2021. We can see that the invasion on Ganquan Island was more severe than that on the Bei Island with five times of *Cassytha filiformis* area. The distribution of *Cassytha filiformis* in the Bei Island was

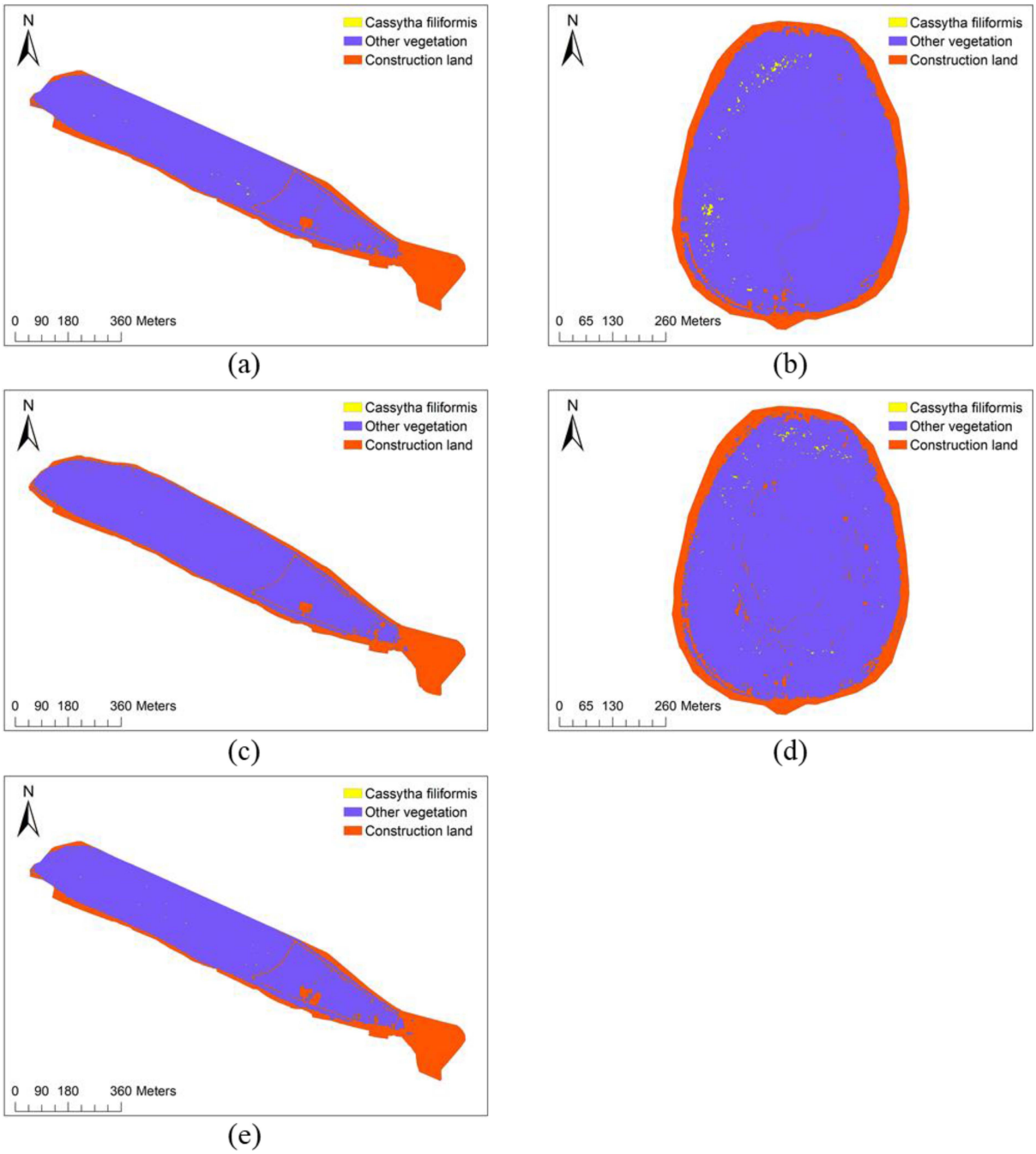

Fig. 10. Classification results for (a) Bei Island in April 2021, (b) Ganquan Island in April 2021, (c) Bei Island in July 2021, (d) Ganquan Island in July 2021, and (e) Bei Island in April 2020.

shown in Fig. 10. In April 2020, it was mainly distribution in the northwestern regions with very small patches. Meanwhile, the distribution of *Cassytha filiformis* decreased in the northwest region, and increased in the central and eastern-central regions in April 2021, especially in the east-central region, the distribution of *Cassytha filiformis* has increased significantly. However, in July 2021, *Cassytha filiformis* in Bei Island was hardly visible in Fig. 10 without zooming in. In contrast, *Cassytha filiformis* was widespread in Ganquan Island, especially along the western and northern edges of the circular forest zone (see Fig. 10). When comparing the distribution of *Cassytha filiformis* in Ganquan Island between April and July 2021, it was observed that the distribution of *Cassytha filiformis* in July decreased in the southwest region and increased in the north region. It suggests that the distribution of *Cassytha filiformis* on the islands is not fixed and will change over time. Combining this information with Fig. 4, it is evident that the primary host of *Cassytha filiformis* in Bei Island was Scaevola sericea Vahl, while in Ganquan Island, the main hosts are Guettarda speciosa L., Scaevola sericea Vahl, and Messerschmidia argentea. Notably, *Cassytha filiformis* has a more extensive range of hosts on Ganquan Island compared to Bei Island.

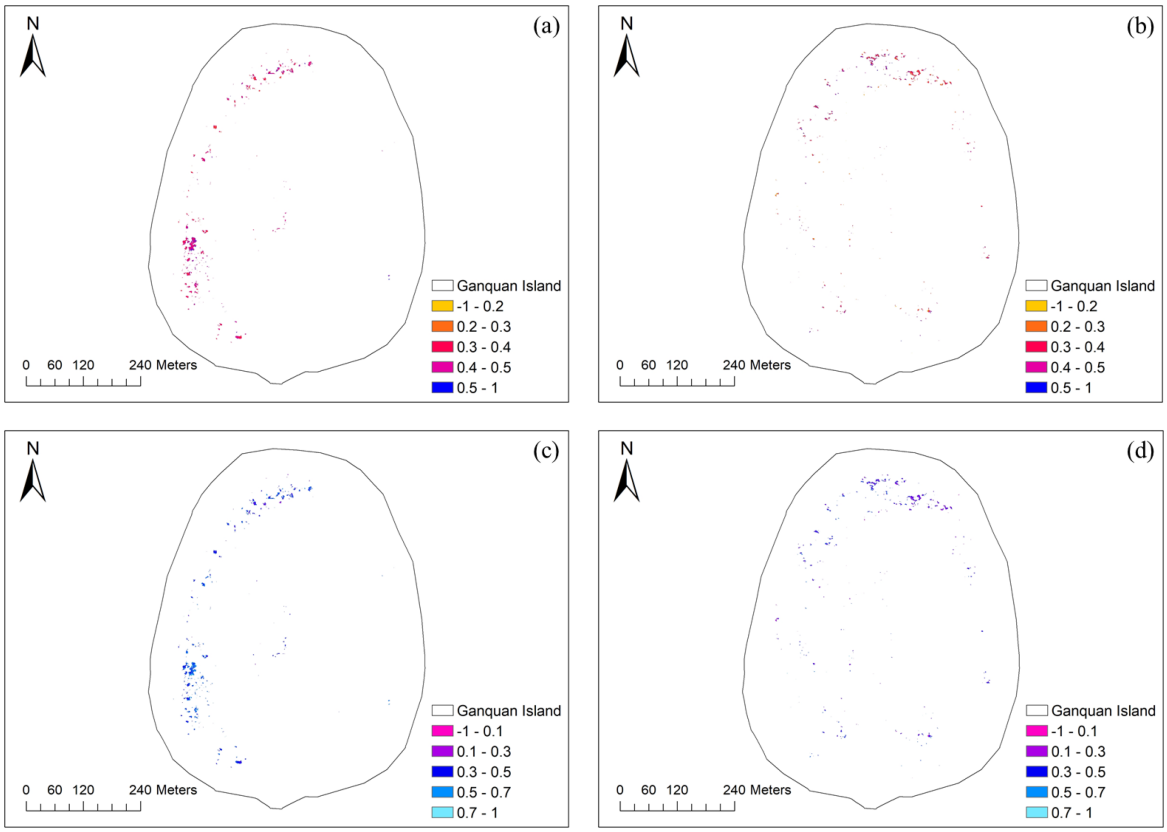

Fig. 11. Vegetation index values for *Cassytha filiformis* on Ganquan Island. (a) GNDVI in April 2021. (b) GNDVI in July 2021. (c) NDVI in April 2021. (d) NDVI in July 2021.

C. Contrasting Invasion Abilities of Cassytha Filiformis in the Wet and Dry Seasons

According to the monitoring results, it is evident that *Cassytha filiformis* exhibits better growth during the dry season (April 2021) on Xisha Islands. To further check this conclusion, Ganquan Island, where the invasion phenomenon of *Cassytha filiformis* is more pronounced, was selected for further study. We decided to use the NDVI and GNDVI indices to assess the vegetation's health and growth status. The NDVI is a well-established tool for measuring the health and vigor of vegetation. The GNDVI offers an enhanced version of NDVI by emphasizing the green part of the spectrum, which can be particularly useful for assessing specific types of vegetation. We extracted the *Cassytha filiformis* patches from the classification results to calculate the NDVI and GNDVI indices (see Fig. 11) to analyze their growing status. Fig. 12 shows that both index values of *Cassytha filiformis* are significantly higher in April (GNDVI = 0.4±0.08 and NDVI = 0.48±0.12) than those in July (GNDVI = 0.36±0.15 and NDVI = 0.36±0.18). We also calculated the NDVI and GNDVI indices of other vegetation types (see Fig. 12) and found that both index values are significantly lower in the dry season than those in the wet season. This indicates that only *Cassytha filiformis* has better growth status in the dry season which is consistent with the prevailing phenomenon of its invasion.

To further investigate why the dry season is more favorable for the growth of *Cassytha filiformis*, we selected four typical climatic parameters: temperature, precipitation, wind speed and potential evapotranspiration to find the climate drivers. The variables were acquired in April and July 2021, to analyze their influence on the growth of *Cassytha filiformis*.

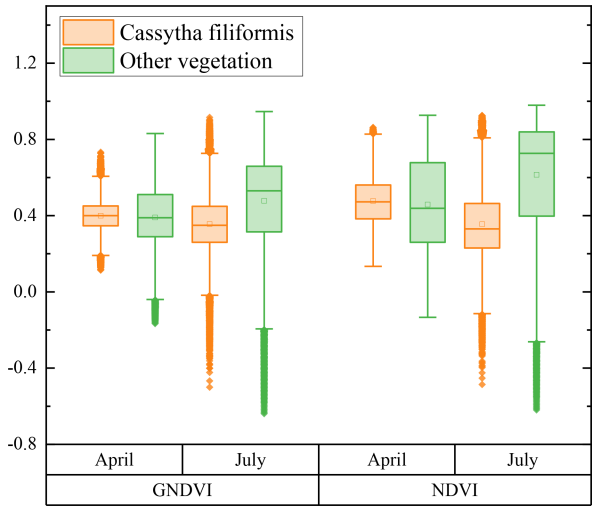

Fig. 12. Boxplot of NDVI and GNDVI values for *Cassytha filiformis* and other vegetation on Ganquan Island in 2021. The box represents the interquartile range, the horizontal line Inside the box indicates the median, and discrete points indicate outliers, with upper and lower whiskers representing the upper and lower quartiles of the data.

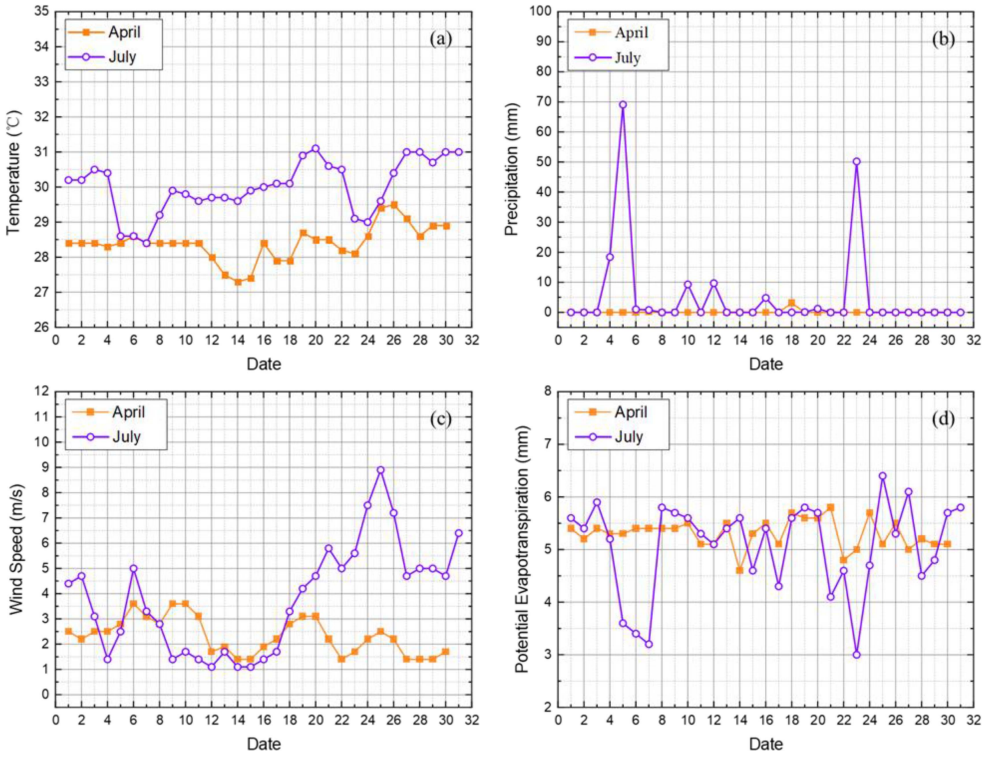

Fig. 13. Meteorological parameters of the study area in April 2021, July 2021. (a) Daily mean temperature, (b) daily precipitation. (c) Daily mean wind speed. (d) Daily potential evapotranspiration.

The results are presented in Fig. 13. In April 2021 (dry season), the monthly mean temperature is 1.6°C lower compared to July 2021 (wet season), with a noticeable difference in the middle of the month, as depicted in Fig. 13(a). The lower temperature during the dry season can promote moisture accumulation, leading to a relatively wetter climate [39]. Precipitation in the Xisha Islands is significantly higher in July 2021 (164.6 mm) compared to April 2021 (4.2 mm) [see Fig. 13(b)]. The decrease in precipitation during the dry season can worsen the soil water deficit. Additionally, the monthly mean wind speed is lower in April 2021 (2.3 m/s) than in July 2021 (3.8 m/s) in the Xisha Islands [see Fig. 13(c)]. The decrease in wind speed during the dry season may help alleviate the soil water deficit [40]. Furthermore, as shown in Fig. 13(d), there is little difference in potential evapotranspiration between April 2021 (5.3 mm) and July 2021 (5.07 mm) in the Xisha Islands.

To provide a more concise comparison of the climate, we calculated the relative MI. The results indicate the relative MI in the Xisha Islands was −0.98 in April 2021 (dry season) and 0.04 in July 2021 (wet season). This suggests that the climate during the dry season is arid. Therefore, we can speculate that *Cassytha filiformis* prefers arid climates, which explains its robust growth during the dry season.

IV. Discussion

Monitoring results in Section III-B show an upward trend in *Cassytha filiformis* area on the Bei Island from 211.8 m^2 in April 2020 to 458.6 m^2 in April 2021. Because of basically uninhabited in the Bei Island, climate change is the main reason for species invasion. Considering a major El Niño event in the eastern and central equatorial Pacific from winter 2019 to spring 2020 (the ONI phase is shown in Fig. 14(e) changed from positive to negative to a La Niña event in May 2020), climate anomalies in 2020 could be responsible for the spread of *Cassytha filiformis* invasion. To test this hypothesis, we inspected the variation of four meteorological parameters (Temperature, precipitation, wind speed and potential evapotranspiration) in April 2020 and 2021.

By analyzing the meteorological parameters, we speculate that *Cassytha filiformis* prefers arid climate. As is shown in Fig. 14(a), the temperature in April 2021 is higher than that of the same period in 2020, and the monthly mean temperature (28.4 °C) is slightly higher than that in 2020 (27.8 °C). Moderate warming may have a positive effect on increasing vegetation activities [41]. The difference in precipitation between the two years is only 10 mm [see Fig. 14(b)], and the April 2021 precipitation is slightly lower than the 2020 precipitation. In Fig. 14(c), the variation curve of monthly wind speed in April 2021 is much lower than that in April 2020. The monthly mean wind speed in April 2021 is 2.32 m/s, which is much lower than the 5.62 m/s in April 2020. However, as shown in Fig. 14(d), the monthly mean potential evapotranspiration in April 2021 is 5.3 mm, which is higher than that of the same period in 2020 (4.88 mm). The variations of temperature, precipitation, wind speed and potential evapotranspiration were inconsistent. Therefore, we also calculated the relative MI and results show that the relative MI in April 2021 (−0.98) is lower than in April

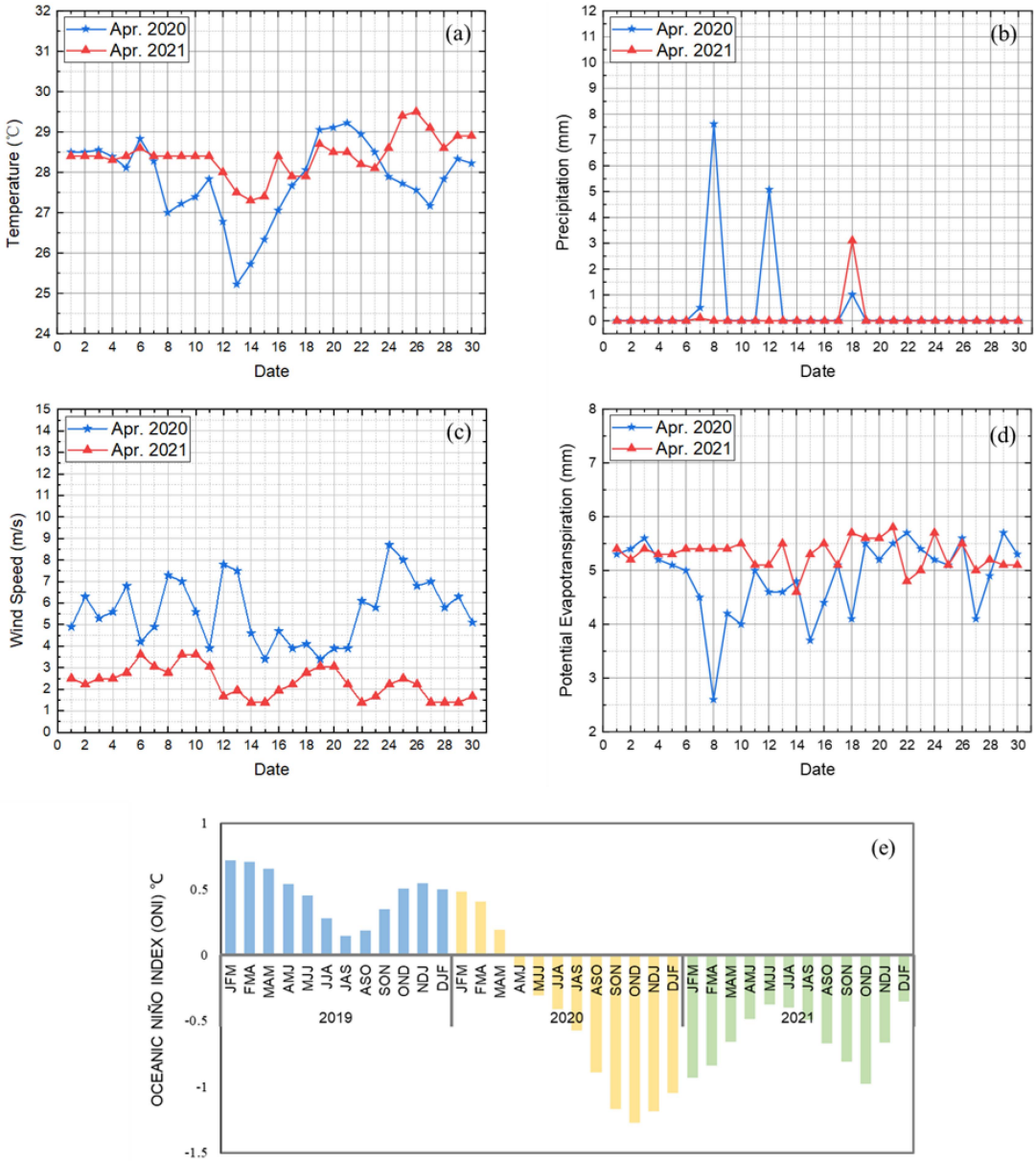

Fig. 14. Meteorological parameters of the study area in April 2020 and 2021. (a) Daily mean temperature. (b) Daily precipitation. (c) Daily mean wind speed. (d) Daily potential evapotranspiration. (e) ONI during 2019-2021, JFR is an acronym using the first letters of January through March, with other acronyms following the same pattern.

2020 (−0.90). The lower value reflects a relatively arid climate which as mentioned above is favorable for *Cassytha filiformis* to growth. This suggests that El Niño causes abnormal weather in 2020, drier condition in April 2021 is responsible for the expansion of *Cassytha filiformis* in 2021.

Many studies have shown that *Cassytha filiformis* is widely distributed in tropical islands, in coastal habitats and has many hosts [42], [43], [44], [45]. Its seeds can be dispersed by birds, water currents and strong winds [6]. It suggests that this may be the reason why signs of invasion by *Cassytha filiformis* have been found on both Bei Island and Ganquan Island. Meanwhile, Zhang et al. also reporte the phenomenon of *Cassytha filiformis* invasion in Xisha Islands [46]. At present, there is little research on the climate driving factors of *Cassytha filiformis* growth. Zhang et al. [46] has found that both temperature and precipitation will affect the growth of *Cassytha filiformis*. Zamora and Buriyo has found that the probability of a host being parasitized by *Cassytha filiformis* is significantly lower at high latitudes than at low latitudes [47], [48]. The results of our study confirm the influence of meteorological factors on the growth of *Cassytha filiformis*. In addition, we find that arid climatic condition is the key factor affecting the growth of *Cassytha filiformis*, which will provide new ideas for the control of *Cassytha filiformis*. While our results align with previous studies, a lack of UAV data from other years prevented further verification of our findings. Additionally, when expanding the factors influencing *Cassytha filiformis*, we only discussed climatic factors, which has certain limitations.

V. Conclusion and Discussions

The Xisha Islands are small and cloudy all year round, and therefore it is not easy to obtain optical satellite images to implement timely monitoring. In this article, we use DJI 4 multispectral UAV imagery combined with a deep learning classification model to monitor the invasion of *Cassytha filiformis* on the Bei Island and Ganquan Island. We can draw the following conclusions.

1) Multispectral UAV images and deep learning methods are powerful tools to monitor *Cassytha filiformis* invasion in small tropical islands.
2) Both Bei Island and Ganquan Island have been invaded by *Cassytha filiformis* and the invasion in Ganquan Island is more severe.
3) *Cassytha filiformis* favors the dry season, and a dry climate can also cause the expansion of this species.

Our study successfully demonstrated the efficacy of employing UAV imagery in conjunction with a deep learning model to monitor the invasion of *Cassytha filiformis*. This approach introduces a novel method for plant invasion monitoring. Additionally, our findings regarding the preference of *Cassytha filiformis* for arid climates present a new avenue for controlling their spread. In the future, we will further investigate the growth changes of *Cassytha filiformis* in different years to figure effective measures to prevent the invasion of *Cassytha filiformis*.

Acknowledgment

Tong Yu, Jiankang Shi, and Xiaohui Sun provided data and some results. Yuhan Xie and Tong Yu developed the method. Yuhan Xie wrote the manuscript. Wenjin Wu and Xinwu Li reviewed the manuscript by rewriting, discussing, and commenting. All authors contributed to the manuscript and approved the submitted version.

References

[1] S. C. Nelson, "Cassytha filiformis," *College Trop., Agriculture Hum. Resour., Univ. Hawai Plant Dis.*, vol. 42, pp. 1–10, 2008.
[2] S. Mythili, S. Gajalakshmi, A. Sathiavelu, and T. Sridharan, "Pharmacological activities of Cassytha filiformis: A review," *Asian J. Plant Sci. Res.*, vol. 1, no. 1, pp. 77–83, 2011.
[3] G. Kokubugata and M. Yokota, "Host specificity of Cassytha filiformis and C. pergracilis (Lauraceae) in the Ryukyu Archipelago," *Bull. Nat. Museum Nature Sci.*, vol. 38, no. 2, pp. 47–53, 2012.
[4] P. Thang, N. Vien, and T. Khanh, "Allelopathic potential of an invasive plant (Cassytha filiformis L.) under different assessing conditions," *Plant Cell Biotechnol.*, vol. 22, no. 17/18, pp. 82–94, 2021.
[5] M. Abubacker, M. Prince, and Y. Hariharan, "Histochemical and biochemical studies of parasite–host interaction of Cassytha filiformis Linn. and Zizyphus jujuba Lamk," *Curr. Sci.*, vol. 89, no. 12, pp. 2156–2159, 2005.
[6] S. Rohani, A. L. Teh, and M. R. Salam, "Parasitic plants at the coastal of Setiu, Terengganu: Distribution and its association with host trees," *Greater Kenyir Landscapes, Social Develop. Environ. Sustainability, Ridge Reef*, pp. 91–100, 2019.
[7] B. R. Kidunda, L. J. Kasuga, and G. Alex, "Assessing the existence spread and control strategies of parasitic weed (Cassytha filiformis) on cashew trees in Tanzania," *J. Adv. Agricultural Technol.*, vol. 4, no. 3, pp. 285–289, 2017.
[8] P. Carr, T. Wilkinison, and S. Barrios, "British Indian Ocean Territory ecosystem action plan," 2020.
[9] N. C. Hoi and V. H. Dang, "Environmental issues in the South China Sea: Legal obligation and cooperation drivers i," *Int. J. Law Public Admin.*, vol. 1, no. 1, pp. 8–23, 2018.
[10] Y. Tong, S. Jian, Q. Chen, Y. Li, and F. Xing, "Vascular plant diversity of the Paracel Islands, China," *Biodiversity Sci.*, vol. 21, no. 3, pp. 364–374, 2013.
[11] H. Cai, H. Lu, Y. Tian, Z. Liu, Y. Huang, and S. Jian, "Effects of invasive plants on the health of forest ecosystems on small tropical coral islands," *Ecol. Indicators*, vol. 117, 2020, Art. no. 106656.
[12] P. Pyšek, V. Jarošík, P. E. Hulme, J. Pergl, M. Hejda, and U. Schaffner, "A global assessment of invasive plant impacts on resident species, communities and ecosystems: The interaction of impact measures, invading species' traits and environment," *Glob. Change Biol.*, vol. 18, no. 5, pp. 1725–1737, 2012.
[13] M. Vilà, J. L. Espinar, M. Hejda, P. E. Hulme, and P. Pyek, "Ecological impacts of invasive alien plants: A meta-analysis of their effects on species, communities and ecosystems," *Ecol. Lett.*, vol. 14, no. 7, pp. 702–708, 2011.
[14] P. M. Vitousek, "Biological invasions and ecosystem processes: Towards an integration of population biology and ecosystem studies," *Oikos*, vol. 57, pp. 7–13, 1990.
[15] S. Reinermann, S. Asam, and C. Kuenzer, "Remote sensing of grassland production and management—A review," *Remote Sens.*, vol. 12, no. 12, 2020, Art. no. 1949.
[16] B. W. Pengra, C. A. Johnston, and T. R. Loveland, "Mapping an invasive plant, Phragmites australis, in coastal wetlands using the EO-1 Hyperion hyperspectral sensor," *Remote Sens. Environ.*, vol. 108, no. 1, pp. 74–81, 2007.
[17] G. A. Carter et al., "Remote sensing and mapping of tamarisk along the Colorado river, USA: A comparative use of summer-acquired Hyperion, Thematic Mapper and QuickBird data," *Remote Sens.*, vol. 1, no. 3, pp. 318–329, 2009.
[18] B. A. Bradley and J. F. Mustard, "Characterizing the landscape dynamics of an invasive plant and risk of invasion using remote sensing," *Ecol. Appl.*, vol. 16, no. 3, pp. 1132–1147, 2006.
[19] M. Liu et al., "Rapid invasion of Spartina alterniflora in the coastal zone of Mainland China: New observations from Landsat OLI images," *Remote Sens.*, vol. 10, no. 12, 2018, Art. no. 1933.
[20] M. Kimothi and A. Dasari, "Methodology to map the spread of an invasive plant (Lantana camara L.) in forest ecosystems using Indian remote sensing satellite data," *Int. J. Remote Sens.*, vol. 31, no. 12, pp. 3273–3289, 2010.
[21] P. L. Raeva, J. Šedina, and A. Dlesk, "Monitoring of crop fields using multispectral and thermal imagery from UAV," *Eur. J. Remote Sens.*, vol. 52, no. 1, pp. 192–201, 2019.
[22] J. A. Berni, P. J. Zarco-Tejada, L. Suárez, and E. Fereres, "Thermal and narrowband multispectral remote sensing for vegetation monitoring from an unmanned aerial vehicle," *IEEE Trans. Geosci. Remote Sens.*, vol. 47, no. 3, pp. 722–738, Mar. 2009.
[23] W. van Iersel, M. Straatsma, E. Addink, and H. Middelkoop, "Monitoring height and greenness of non-woody floodplain vegetation with UAV time series," *Int. Soc. Photogramm. Remote Sens. J. Photogramm. Remote Sens.*, vol. 141, pp. 112–123, 2018.
[24] Y. Lu, D. Macias, Z. S. Dean, N. R. Kreger, and P. K. Wong, "A UAV-mounted whole cell biosensor system for environmental monitoring applications," *IEEE Trans. Nanobiosci.*, vol. 14, no. 8, pp. 811–817, Dec. 2015.
[25] J. A. Goncalves and R. Henriques, "UAV photogrammetry for topographic monitoring of coastal areas," *Int. Soc. Photogramm. Remote Sens. J. Photogramm. Remote Sens.*, vol. 104, pp. 101–111, 2015.
[26] S. Verykokou, A. Doulamis, G. Athanasiou, C. Ioannidis, and A. Amditis, "UAV-based 3D modelling of disaster scenes for urban search and rescue," in *Proc. IEEE Int. Conf. Imag. Syst. Techn.*, 2016, pp. 106–111.
[27] A. C. Watts, V. G. Ambrosia, and E. A. Hinkley, "Unmanned aircraft systems in remote sensing and scientific research: Classification and considerations of use," *Remote Sens.*, vol. 4, no. 6, pp. 1671–1692, 2012.
[28] K. Anderson and K. Gaston, "Lightweight unmanned aerial vehicles will revolutionize spatial ecology," *Front. Ecol. Environ.*, vol. 11, no. 3, pp. 138–146, 2013.
[29] S. Candiago, F. Remondino, M. De Giglio, M. Dubbini, and M. Gattelli, "Evaluating multispectral images and vegetation indices for precision farming applications from UAV images," *Remote Sens.*, vol. 7, no. 4, pp. 4026–4047, 2015.
[30] J. Lopatin, K. Dolos, T. Kattenborn, and F. E. Fassnacht, "How canopy shadow affects invasive plant species classification in high spatial resolution remote sensing," *Remote Sens. Ecol. Conservation*, vol. 5, no. 4, pp. 302–317, 2019.
[31] DJI, 2020. [Online]. Available: https://dl.djicdn.com/downloads/p4-multispectral/20200717/P4_Multispectral_Image_Processing_Guide_CHS.pdf

[32] Z. D., 2021. [Online]. Available: https://zhuanlan.zhihu.com/p/352965698
[33] A. A. Gitelson, Y. J. Kaufman, and M. N. Merzlyak, "Use of a green channel in remote sensing of global vegetation from EOS-MODIS," *Remote Sens. Environ.*, vol. 58, no. 3, pp. 289–298, 1996.
[34] C. J. Tucker, "Red and photographic infrared linear combinations for monitoring vegetation," *Remote Sens. Environ.*, vol. 8, no. 2, pp. 127–150, 1979.
[35] N. Pettorelli, W. F. Laurance, T. G. O'Brien, M. Wegmann, H. Nagendra, and W. Turner, "Satellite remote sensing for applied ecologists: Opportunities and challenges," *J. Appl. Ecol.*, vol. 51, no. 4, pp. 839–848, 2014.
[36] J. W. Rouse, R. H. Haas, J. A. Schell, and D. W. Deering, "Monitoring vegetation systems in the great plains with ERTS," *Nat. Aeronaut. Space Admin. Special Publication*, vol. 351, no. 1, p1974.
[37] D. A. García Cárdenas, J. A. Ramón Valencia, D. F. A. Velásquez, and J. R. P. Gonzalez, "Dynamics of the indices NDVI and GNDVI in a rice growing in its reproduction phase from multi-spectral aerial images taken by drones," in *Proc. Int. Conf. ICT Adapting Agriculture Climate Change*, 2018, pp. 106–119.
[38] T. Yu, W. Wu, C. Gong, and X. Li, "Residual multi-attention classification network for a forest dominated tropical landscape using high-resolution remote sensing imagery," *Int. Soc. Photogramm. Remote Sens. Int. J. Geo-Inf.*, vol. 10, no. 1, 2021.
[39] E. Tello-García, L. Huber, G. Leitinger, A. Peters, and E. Tasser, "Drought- and heat-induced shifts in vegetation composition impact biomass production and water use of alpine grasslands," *Environ. Exp. Botany*, vol. 169, 2020, Art. no. 103921.
[40] M. Mahmoodabadi and H. Rajabpour, "Study on the effect of initial soil moisture content on wind erosion rate using a laboratory wind tunnel," *J. Water Soil Conservation*, vol. 24, no. 2, pp. 167–183, 2017.
[41] W. Lucht, "Climatic control of the high-latitude vegetation greening trend and Pinatubo effect," *Science*, vol. 296, no. 5573, pp. 1687–1689, 2002.
[42] A. A. Ambi, G. F. Nuru, A. T. Mora, and A. Ahmad, "Pharmacognostic studies and elemental analysis of Cassytha filiformis Linn," *J. Pharmacognosy Phytotherapy*, vol. 9, no. 8, pp. 131–137, 2017.
[43] A. C. Giannerini, A. Quinet, and R. H. P. Andreata, "Lauraceae no Parque Nacional do Itatiaia, Brasil," *Rodrigusia*, vol. 66, no. 3, pp. 863–880, 2015.
[44] D. Debabrata, "Cassytha filiformis in forests of Jhargram district of West Bengal," *GSC Biol. Pharmaceut. Sci.*, vol. 4, no. 1, pp. 1–7, 2018.
[45] C. Werth, W. Pusateri, W. Eshbaugh, and T. Wilson, "Field observations on the natural history of Cassytha filiformis L.(Lauraceae) in the Bahamas," in *Proc. 2nd Int. Symp. Parasitic Weeds*, pp. 94–102, 1979.
[46] H. Zhang, S. Florentine, and K. U. Tennakoon, "The angiosperm stem hemiparasitic genus Cassytha (Lauraceae) and its host interactions: A review," *Front. Plant Sci.*, vol. 13, 2022, Art. no. 864110.
[47] R. Zamora and A. Mellado, "Identifying the abiotic and biotic drivers behind the elevational distribution shift of a parasitic plant," *Plant Biol.*, vol. 21, no. 2, pp. 307–317, 2019.
[48] A. S. Buriyo, L. Kasuga, H. N. Moshi, and W. A. Nene, "Ecological distribution and abundance of the parasitic weed, Cassytha filiformis L.(Lauraceae) in major cashew, Anacardium occidentale L. growing regions in Tanzania," *Int. J. Basic Appl. Sci.*, vol. 5, no. 3, pp. 109–116, 2015.

Yuhan Xie received the bachelor's degree in cartography and geographic information systems from Chang'an University, Xi'an, China, in 2017. She is currently working toward the Doctoral degree with the University of Chinese Academy of Sciences, Beijing, China.

Her research interests are deep learning and vegetation remote sensing.

Wenjin Wu received the B.E. degree in remote sensing science and technology from Wuhan University, Wuhan, China, in 2010 and the Ph.D. degree from the Institute of Remote Sensing and Digital Earth, Chinese Academy of Sciences (CAS), Beijing, China, in 2015.

She is currently an Associate Professor of Aerospace Information Research Institute (AIR), CAS, and the author of more than 60 academic papers. Her research interests include vegetation remote sensing, deep learning, and SAR data processing.

Xinwu Li received the Ph.D. degree from the Institute of Remote Sensing and Digital Earth, Chinese Academy of Sciences (CAS), Beijing, China, in 2002.

He is currently a Professor of AIR, CAS. He was a Visiting Scientist with Natural Resource of Canada and University of Rennes 1, Rennes, France. He has authored or coauthored more than 100 of papers in relevant areas. His current research interests include Global change remote sensing and SAR tomography.

Jiankang Shi received the master's degree in cartography and geographic information systems from the University of Chinese Academy of Sciences, Beijing, China, in 2008.

He is currently a Senior Engineer with Hainan Academy Research of Environmental Sciences, Haikou, China. His main research interests include remote sensing monitoring of ecological environment.

Tong Yu received the master's degree in cartography and geographic information systems from the University of Chinese Academy of Sciences, Beijing, China, in 2021. He is currently working toward the Doctoral degree with the University of Wisconsin-Madison, Madison, WI, USA.

His research interests include remote sensing, machine learning, and precision agriculture.

Xiaohui Sun received the master's degree from Aerospace Information Research Institute, Chinese Academy of Science, Beijing, China, in 2020.

She is currently an Engineer with Qilu Aerospace Information Research Institute, JiNan, China. Her main research interests include remote sensing image analysis and remote sensing of ecological environment.